KRZYSZTOF KRAUZE [1*], RYSZARD KLEMPKA [1],
KAMIL MUCHA [1], TOMASZ WYDRO [1]

COMPUTER-AIDED SELECTION OF THE STABILISING SYSTEM PARAMETERS OF THE MOBILE TRANSPORT AND ASSEMBLY MANIPULATOR IN MINING EXCAVATIONS

Shifting masses in a confined space in the company of other machines and devices, which limits the manoeuvring and transport area, poses a significant problem in every field of industry, especially with underground mining. The works involved in transporting and manoeuvring masses in underground workings are challenging and are most often performed using various auxiliary machines or manually. Hence the need arose to develop a device carrying out activities related to the shifting of masses with the assumed maximum value. The device was created as a result of cooperation between FAMA sp. z o.o. and the AGH University of Science and Technology in Kraków, Poland. The mining modular transport and assembly unit (MZT-M) enables assembling and transporting various masses, especially the elements of the roadway support in the face. The primary function of this device is its movement in the excavation along with the transported mass and delivering it to a specific place. Therefore, an important issue is to ensure the module's stability in different phases of its operation (lifting, transport, manoeuvring, feeding, lowering) due to the limited space in the excavation. That is why an analytical model and specialised software were created to determine the design parameters of the device as a function of its operating phases, especially the counterweight's mass. As previously mentioned, an analytical model (physical, mathematical) with equations and applications written in Microsoft Visual Studio and Matlab was used for this purpose. It is beneficial at the design or construction changes stage. Calculation results are documented in the form of numerical summaries and graphs.

Keywords: underground mining; transport and assembly manipulator; physical model; mathematical model; stability; simulation tests

[1] AGH UNIVERSITY OF SCIENCE AND TECHNOLOGY, AL. MICKIEWICZA 30, 30-059 KRAKÓW, POLAND

* Corresponding author: krauze@agh.edu.pl
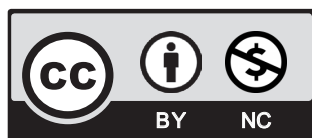
1. Introduction

One of the key processes in underground mines is the driving of workings. The excavation and, later, the exploitation of such a working requires moving various elements of the support, machines and devices included in the equipment used in the face. It is then necessary to use various types of transport devices, stationary or mobile manipulators for this purpose [1,2]. The most difficult thing in such a working, and more precisely in the face, is to transport and install the elements of the roadway support [3] due to very little free space (Fig. 1) [4,5]. This applies to all types of supports, mainly the yielding arch support type ŁP [6,7].

The erection of the frame of the yielding arch support involves mounting its elements in the face with the use of a roadheader [8,9], suspended rails [10] and moving equipment [3]. This process, as can easily be seen, is performed manually, so it is particularly strenuous and requires a lot of physical effort. This applies to the transport of support arches and other elements of the support frame, the lining and the assembly of the support frame itself. Hence the idea to use a device enabling the transport of various masses, including the elements of the support frame, from the place of its storage to the face, in front of the shearer, and their delivery to the place of installation [1,11,12]. Currently, such devices available on the market do not fulfil the above-mentioned functions due to the dimensions of the excavation and the technical equipment of the face (roadheader, conveyors, dust removal devices, ventilation and power supply).

Fig. 1. View of the mining face of a gallery drilled with a roadheader

The concept of using the MZT-M in the mining face has been shown in Fig. 2. The manipulator consists of a boom mounted on a runway beam, a stabilising foot and a hydraulic power pack. The feed drive (tractor) enables the equipment to travel along the track of the suspended monorail (Fig. 2a) [1,13]. When transporting support elements or other masses, the modular transport and assembly unit (MZT-M) must be balanced due to the suspension of the rail on chain strings in the excavation, whether or not this is done symmetrically (transverse and longitudinal stability, the load on the transport beam bogies). Then it is necessary to determine the

value of the counterweight and its location. On the other hand, the operation of the boom itself (manoeuvring) requires stabilising the whole unit, for example, supporting it against the side of the excavation with a stabilising foot (Fig. 2b). However, it is also necessary to determine the longitudinal stability and the load on the transport beam bogies.

Determining the value of the mass needed to balance the device during transport required developing a physical and mathematical model, described in detail in the article [1]. The mathematical model was next used to develop a specialised program enabling a multivariant analysis of the manipulator load and to search for the most favourable solution (payload, design dimensions of the boom, counterweight mass). Hence, the essential purpose of this article is to present the computational capabilities of the above-mentioned computer program and its practical use (kinematics, stability). It is the original part of this article, together with publications [1] and [2]. It should also be noted that the proposed original method of numerical calculations allows for determining the limitations of the analysed device related to the permissible transported masses, stability and operating range.
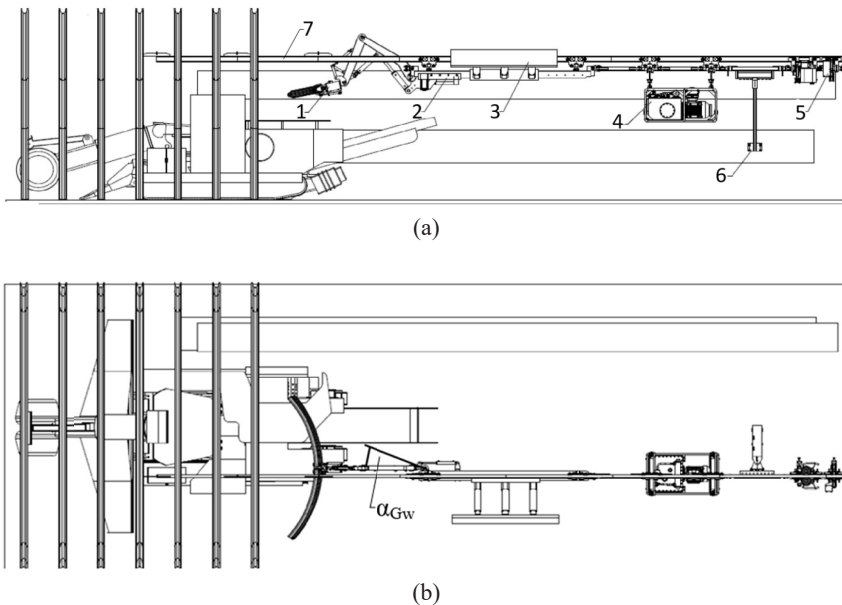

(a)

(b)

Fig. 2. Diagram of the MZT-M in a gallery system with arch in the transport position: a) side view, b) top view: 1 – boom, 2 – beam, 3 – support slide, 4 – hydraulic power unit, 5 – CHM-15 tractor, 6 – control panel, 7 – suspended rail [1]

2. Analytical model of the manipulator for determining its stability

Determining the mass of the counterweight of the manipulator in question is related to the process of transporting the support elements or other masses in the excavation. Then, along the entire transport route, the device cannot come into contact with the sides of the excavation

(arch support) and other objects located in it. On the other hand, the work of the device at the place of shifting (supplying) the support elements or other masses requires stopping the manipulator and expanding it (stabilising). Hence, in both cases, the balance of the device is disturbed, and the required location, especially in the transport position, is lost as a result of changing the position of the boom and the supporting structure of the counterweight and stabiliser [14,15].

As mentioned before, the starting point was a creation of a physical and mathematical model of the manipulator [1]. For this purpose, the boom model was used. Based on the analytical model, the boom structure and kinematics were considered, and relationships that allowed describing the values important for the assessment of the boom's stability as a function of its construction parameters were determined. The above dependencies enable determining the x_s and y_s coordinates of the manipulator's centre of mass. Next, knowing the location of the centre of mass of the entire boom (x_s, y_s) and its resultant mass G_W, it is possible to determine the counterweight G_{st} (stabilising foot) for the variant of manipulator ride with the payload G_U of up to 650 kg (Fig. 3).

$$G_W = G_{S_1} + G_{R_1} + G_{S_2} + G_{R_2} + G_{S_3} + G_M + G_U \qquad (1)$$

where: G_W – resultant mass (weight), kg; G_{S_1} – mass (weight) of the first actuator, kg; G_{R_1} – mass (weight) of the first arm, kg; G_{S_2} – mass (weight) of the second actuator, kg; G_{R_2} – mass (weight) of the second arm, kg; G_{S_3} – mass (weight) of the third actuator, kg; G_M – mass (weight) of the gripping part, kg; G_U – payload (support arch), kg.
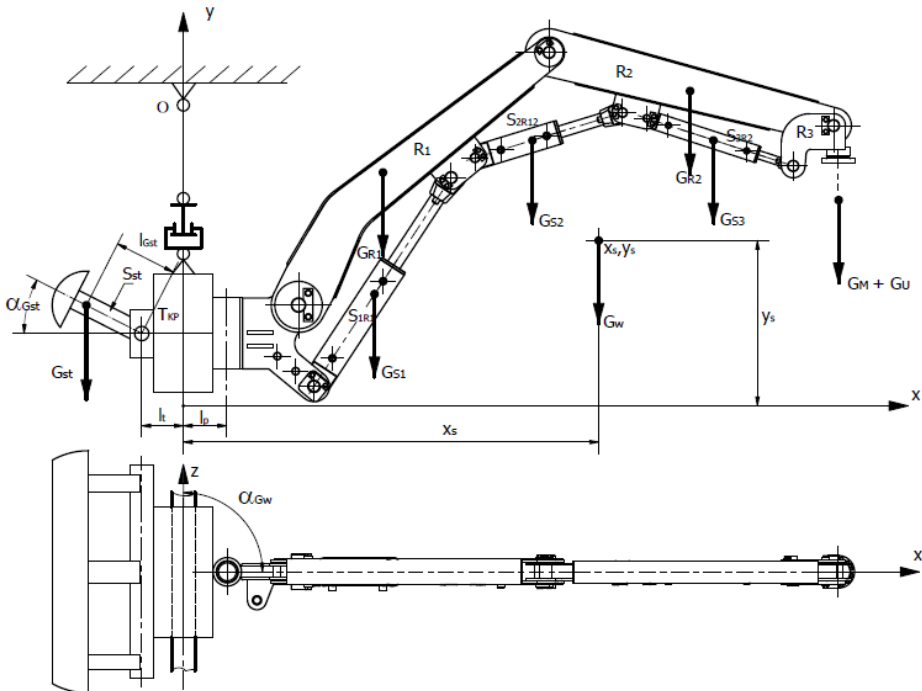

Fig. 3. Diagram of the manipulator in the transport position

$$G_W \cdot x_{st} = G_{st} \cdot l_{Gstt} \tag{2}$$

$$l_{Gstt} = l_{Gst} \cdot \cos\cos\alpha_{Gst} + l_t \tag{3}$$

$$x_{st} = (x_s - l_p) \cdot \sin\sin\alpha_{GW} + l_p \tag{4}$$

$$G_{st} = \frac{G_W \cdot x_{st}}{l_{Gstt}} = G_W \cdot \frac{(x_s - l_p) \cdot \sin\sin\alpha_{GW} + l_p}{l_{Gst} \cdot \alpha_{Gst} + l_t} \tag{5}$$

where: G_{St} – mass (weight) of the stabilising foot, kg; l_{Gst} – length of the arm of the stabilising foot, m.

The above dependencies provide a basis for determining the influence of the manipulator design parameters on its balance (position, stability) during transport (advance speed $v_p \leq 1$ m/min) and its stabilization (advance speed $v_p = 0$ m/min) in the working position. This applies in particular to the mass of the counterweight G_{st}, the boom tilt angle α_{GW} and the length of the stabilizing foot arm l_{Gst}.

It is equally important to determine the load on the transport beam bogies (points A and B), a simplified diagram of which is shown in Fig. 4 (longitudinal stability). Then the beam is loaded with the additional mass (weight) of the hydraulic power unit G_Z and the drive G_n and additionally the mass of the counterweight G_{st}. It is required that the reaction in point A is always positive, and the load on the bogies does not exceed the value resulting from the permissible load of individual support arches (40 kN) to which the rails are suspended [1].
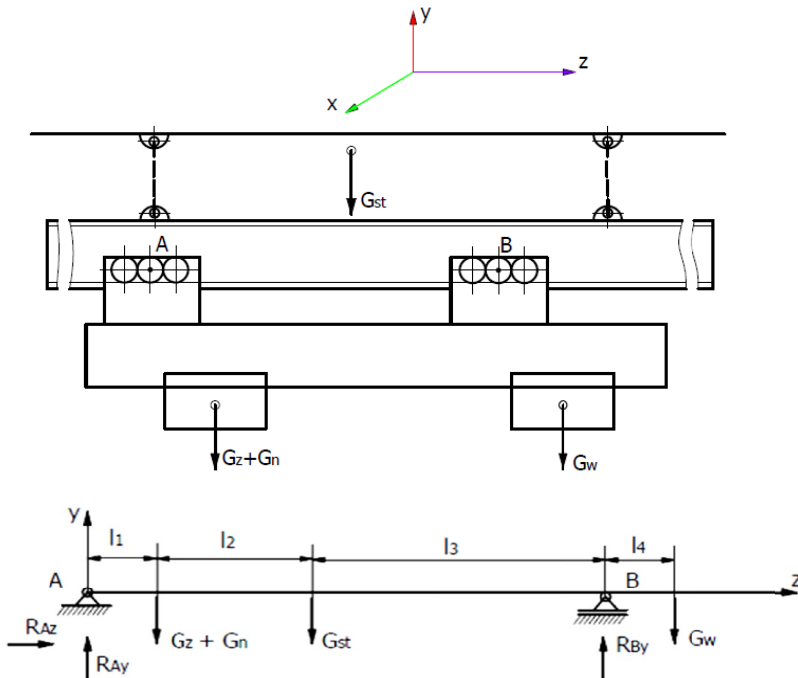

Fig. 4. Simplified diagram of the transport beam loading

Note that the longitudinal stability can be considered correct when the reactions R_{Ay} and R_{By} are positive and each is lower than 40 kN. The value of these reactions (longitudinal stability) is particularly influenced by the distance between them ($l_1 + l_2 + l_3$) and the manipulator's range LZW_z. Hence, it may be necessary to install an additional mass G_{st} for the reaction in support A to be positive.

$$R_{Ay} = G_z + G_n + G_{st} + G_w - R_{By} \tag{6}$$

$$R_{By} = [(G_z + G_n)\, l_1 + G_{st}\, (l_1 + l_2) + G_w\, (l_1 + l_2 + l_3 + l_4)]\, (l_1 + l_2 + l_3)^{-1} \tag{7}$$

3. Characteristics of the computer application

For the purposes of creating a prototype of the manipulator and correcting its dimensions and kinematics, an appropriate application was developed using the created prior analytical model [1]. It enables quick verification of design assumptions in terms of design parameters of individual manipulator elements. Currently, such simulation tests are very commonly used to facilitate the design process and introduce possible model changes [16,17].

The application allows for verifying the impact of changes in the structural dimensions of the manipulator's components on its kinematics and stability. Fig. 5 shows the start-up window of an application written in the Microsoft Visual Studio environment, whereas Fig. 6 presents its main calculation window, also written in the Microsoft Visual Studio environment.

The yellow colour shows the actuator strokes (input data), the counterweight G_{st}, as well as R_{Ay} and R_{By} reaction forces (calculation results). A graphic illustration of the calculation results (boom kinematics) was prepared using an application written in the Matlab environment. The advantage of this environment is the rich set of available functions, while the disadvantage is the large size of the application after its compilation.
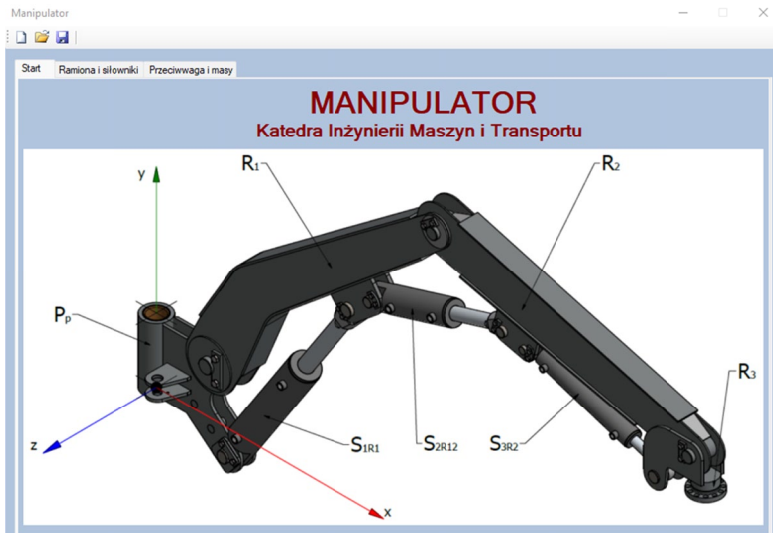

Fig. 5. Application page of the program for determining the manipulator's stability
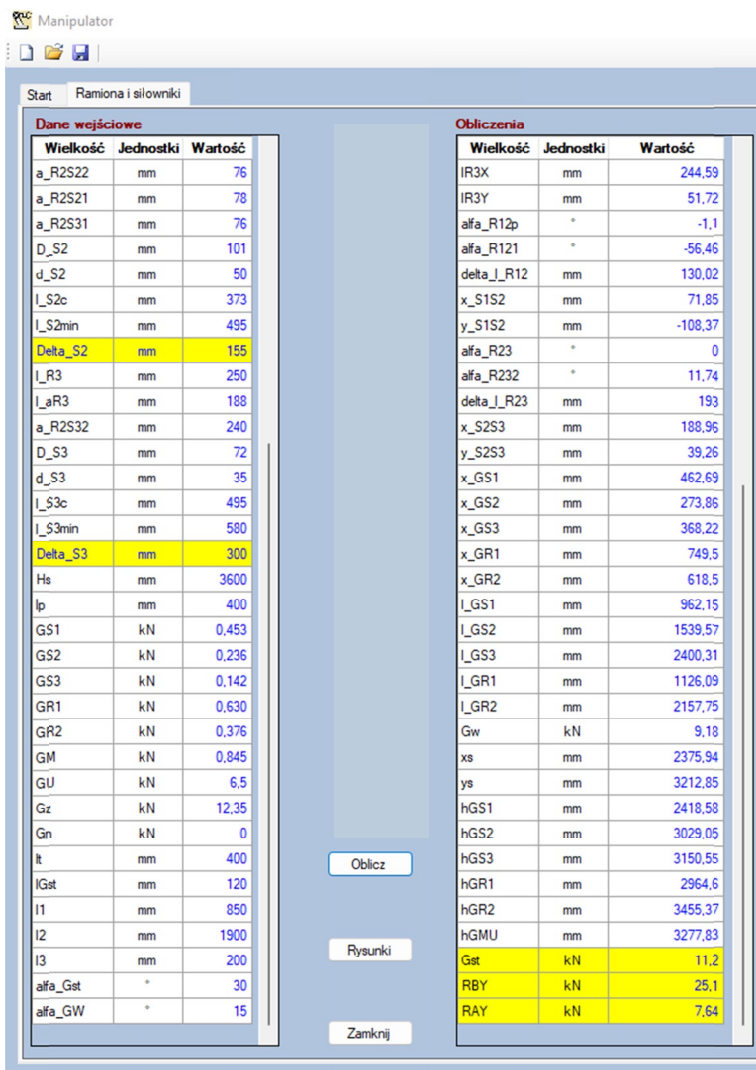
Fig. 6. Main application calculation window with exemplary dimensions in the MS Visual Studio environment

Fig. 7 shows the view of the application written in Matlab for the case of the maximum extension of the actuators. Similarly to the application written in the MS Visual Studio environment, where numerical values are determined, it also enables quick verification of the influence of design parameters on the manipulator's kinematics. Additionally, the graphic application reflects the manipulator's position. In the upper part of the application, three sliders allow changing the degree of extension of each actuator. The application also draws the system of forces for longitudinal stability. It is easy to see that multi-variant calculations are possible. Additionally, security measures have been introduced associated with the introduction of incorrect data, especially design data.
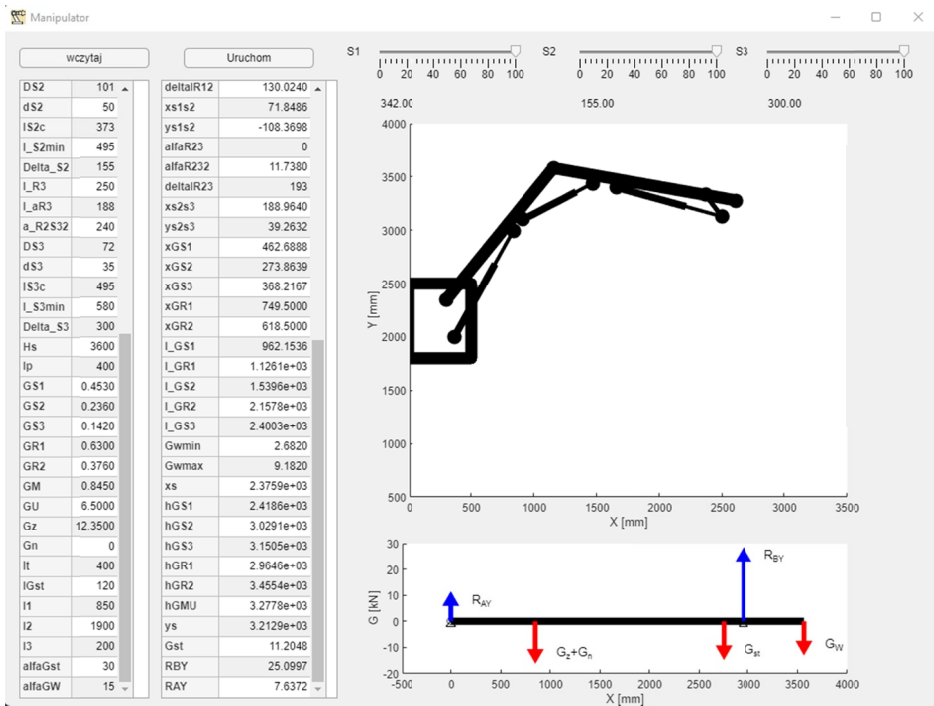
Fig. 7. Exemplary main application calculation window in the MS Visual Studio environment

4. Example of the practical use of the application

The aforementioned applications were utilised to analyse the manipulator's structure while taking into account its two phases of operation. The first analysis concerned the transport phase in an excavation with a payload reaching up to 650 kg, whereas the second one concerned the phase in which this mass is shifted during downtime. First, numerical calculations were carried out using the design data of the manipulator, and then an experiment was carried out on a real object.

As mentioned before, the transport phase requires the manipulator to be balanced so that none of its elements come into contact with the excavation sides or other objects in the roadway during the ride along the rail. In this case, the most advantageous position of the manipulator and its extension arm (transport position) should be determined. Next, the value of the counterweight G_{st}, the arm tilt angle α_{GW} and its length l_{Gst} should be determined for this configuration.

It has been assumed that the manipulator will be suspended at a height of 4 m from the floor (a_{so}) on the left side of the excavation. Of course, for such a system, the trajectory of the manipulator tip movement should be determined for the minimum and maximum strokes of the actuators (l_{s1}, l_{s2}, l_{s3}). It will then allow choosing its most advantageous position from the point of view of the counterweight value. The position of the manipulator in the vertical plane for the minimum and maximum extensions of the actuators has been shown in Figs. 8 and 9, but the maximum manipulator's range has been shown in Fig. 10.
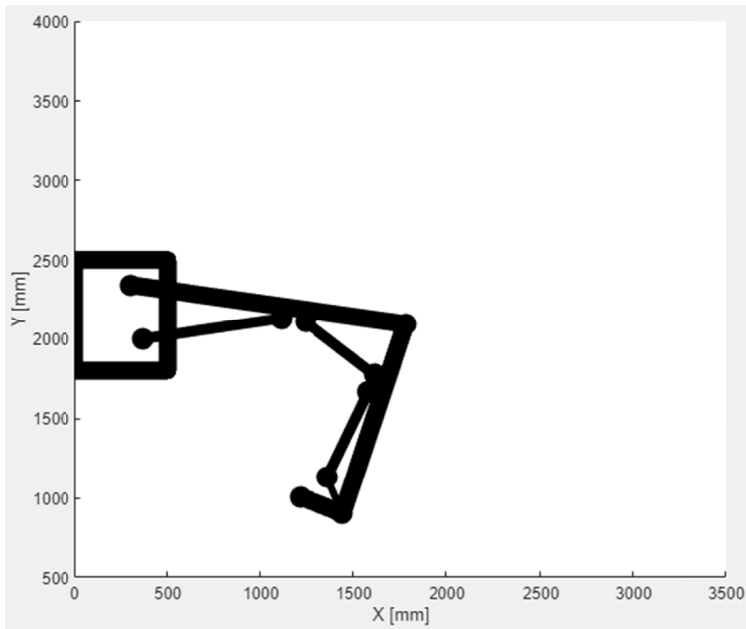
Fig. 8. Movement trajectory of the manipulator tip's movement for the minimal extension of the actuators ($l_{s1} = l_{s2} = l_{s3} = 0$)
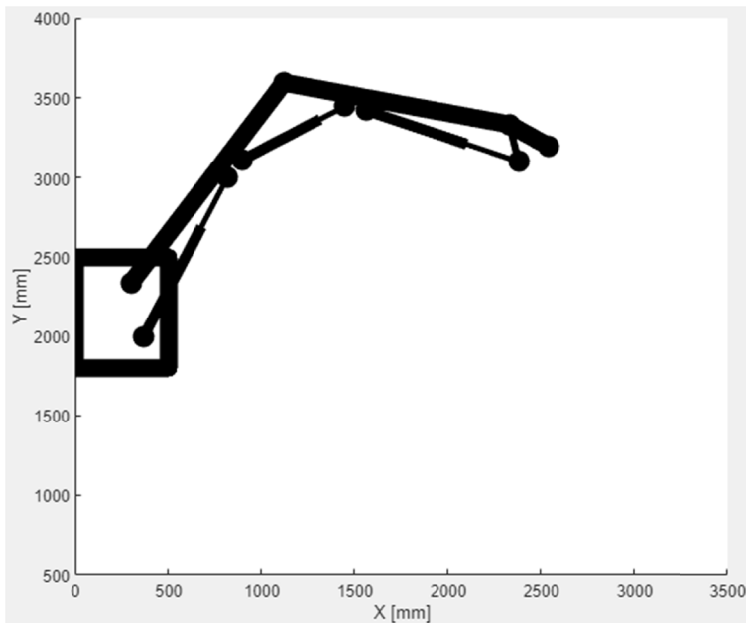

Fig. 9. Movement trajectory of the manipulator tip's movement for the maximum extension of the actuators ($l_{s1} = l_{s1max}$, $l_{s2} = l_{s2max}$, $l_{s3} = l_{s3max}$)
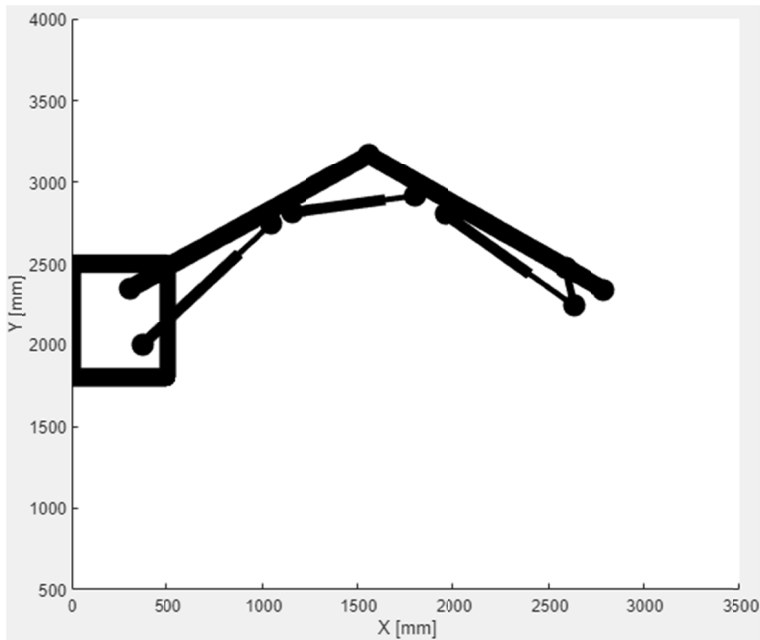
Fig. 10. Movement trajectory of the manipulator tip's movement for its maximum range
$(l_{s1} < l_{s1max}, l_{s2} = l_{s2max}, l_{s3} = l_{s3max})$

Fig. 11 shows the curve of the G_{st} counterweight value as a function of the α_{GW} arm tilt angle for the minimum ($l_{s1} = l_{s1min}, l_{s2} = l_{s2min}, l_{s3} = l_{s3min}$) and maximum ($l_{s1} = l_{s1max}, l_{s2} = l_{s2max}, l_{s3} = l_{s3max}$) extensions of the actuators (LZW_{smin}, LZW_{smax}) and the maximum ($l_{s1} < l_{s1max}, l_{s2} = l_{s2max}, l_{s3} = l_{s3max}$) manipulator range ($LZW_{zmax}$). It turns out that the mass of the counterweight G_{st} (transverse stability), which should be expected taking into account equation (2), increases with the tilting of the manipulator (α_{GW}). Based on these calculations and graphs, it is easy to determine the most favourable value of the counterweight so that the reactions in the R_{Ay} and R_{By} supports have permissible values (up to 40 kN) during the mass transport up to 650 kg. The arm tilt angle cannot be greater than 20°, and the counterweight reached 1500 kg. However, after reaching this angle value, it becomes necessary to stabilise the manipulator with the stabilising foot.

Figs. 12 and 13 show the reaction value curves at points A and B as a function of the trajectory of the manipulator tip movement in the vertical plane for the minimum and maximum extensions of the actuators and the arm tilt angle α_{GW} and for the maximum manipulator's range for the 6-metre distance of trolleys A and B ($l_1 + l_2 + l_3 = 6$ m). Calculations and reaction value curves in points A and B were performed for a 6 m beam, without a drive unit ($G_n = 0$) and with a drive unit ($G_n = 6.85$ kN), where G_{st} value is a function of the arm tilt angle α_{GW}. In both cases, the manipulator obtains the correct longitudinal stability ($R_{Ay} > 0$). During the operational tests, it was found that the 6 m beam is too long for the turning circles of the mine workings, making it difficult for the manipulator to pass and requiring disassembly of its drive unit. It resulted in the necessity to shorten the beam to 2.95 m. As before, appropriate calculations were made, and the longitudinal stability for the manipulator with a beam of 2.95 m was determined (Figs. 14, 15).
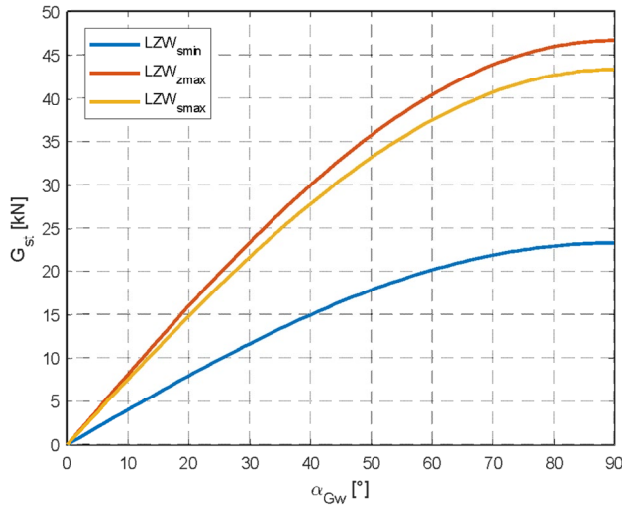
Fig. 11. G_{st} counterweight value curves as a function of the tilt angle α_{GW} for the minimum $LZW_{s\min}$ and maximum $LZW_{s\max}$ extensions of the actuators and for the maximum manipulator's range $LZW_{z\max}$
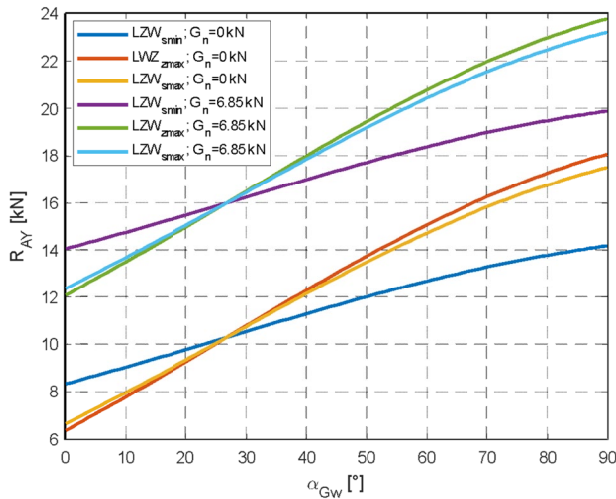

Fig. 12. Reaction value curve at points A as a function of the trajectory of the manipulator tip movement in the vertical plane for the minimum $LZW_{s\min}$ and maximum $LZW_{s\max}$ extensions of the actuators and the arm tilt angle α_{GW} and for the maximum manipulator's range $LZW_{z\max}$, where $G_n = 0$ and $G_n = 6.85$ kN ($l_c = l_1 + l_2 + l_3 = 6$ m)

It turns out that the manipulator, as before, obtains the correct longitudinal stability ($R_{Ay} > 0$) in both cases.

Bearing in mind the transverse stability and the assumed value of the counterweight ($G_{st} = 1500$ kg, $\alpha_{GW} = 20°$) and the passage of the manipulator with a payload ($G_U = 650$ kg), it
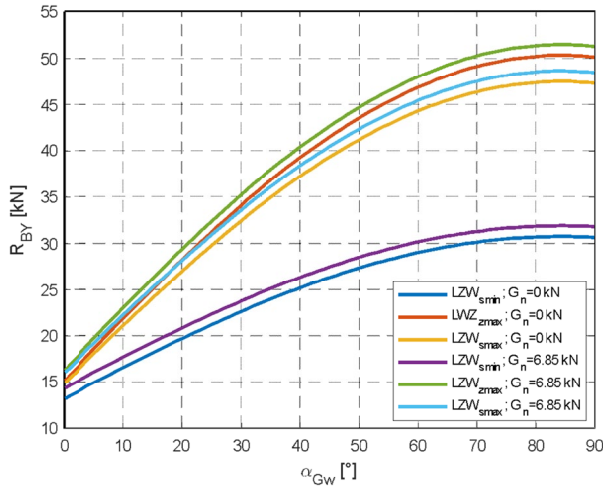
Fig. 13. Reaction value curve at points B as a function of the trajectory of the manipulator tip movement in the vertical plane for the minimum $LZW_{s\min}$ and maximum $LZW_{s\max}$ extensions of the actuators and the arm tilt angle α_{GW} and for the maximum manipulator's range $LZW_{z\max}$, where $G_n = 0$ and $G_n = 6.85$ kN ($l_c = l_1 + l_2 + l_3 = 6$ m)
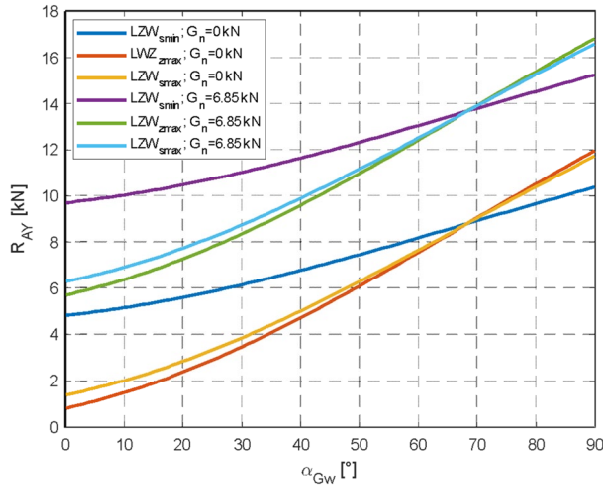

Fig. 14. Reaction value curve at points A as a function of the trajectory of the manipulator tip movement in the vertical plane for the minimum $LZW_{s\min}$ and maximum $LZW_{s\max}$ extensions of the actuators and the arm tilt angle α_{GW} and for the maximum manipulator's range $LZW_{z\max}$, where $G_n = 0$ and $G_n = 6.85$ kN ($l_c = l_1 + l_2 + l_3 = 2.95$ m)

becomes expedient to check the longitudinal stability for this configuration. The results of the calculations are presented in Figs. 16 and 17. As before, the manipulator keeps the correct longitudinal stability, and the reaction values in points A and B (rear bogie A, front bogie B) have positive and permissible values.
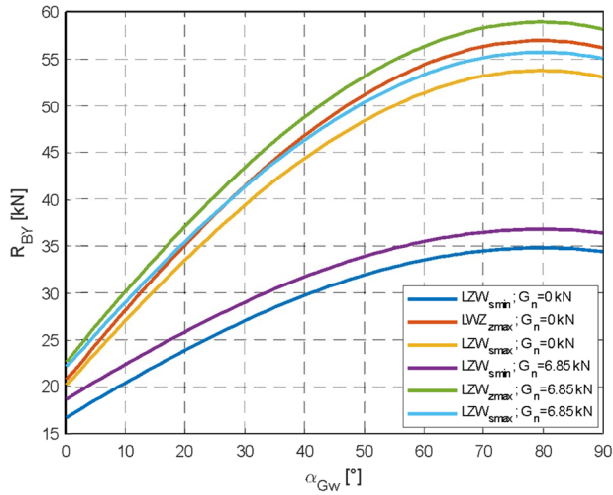
Fig. 15. Reaction value curve at points B as a function of the trajectory of the manipulator tip movement in the vertical plane for the minimum $LZW_{s\,min}$ and maximum $LZW_{s\,max}$ extensions of the actuators and the arm tilt angle α_{GW} and for the maximum manipulator's range $LZW_{z\,max}$, where $G_n = 0$ and $G_n = 6.85$ kN ($l_c = l_1 + l_2 + l_3 = 2.95$ m)

Fig. 16. Reaction value curve at points A as a function of the trajectory of the manipulator tip movement in the vertical plane for the maximum manipulator's range $LZW_{z\,max}$ and the arm tilt angle α_{GW}, where $G_n = 0$ and $G_n = 6.85$ kN ($l_c = l_1 + l_2 + l_3 = 2.95$ m and 6 m)

The above example shows the possibilities of analytically determining the transverse and longitudinal manipulator's stability as a function of its design and mass parameters and determining the counterweight mass value as a function of the arm tilt. Of course, it is also possible to search for other solutions (combinations) that are important due to the requirements of the future user.
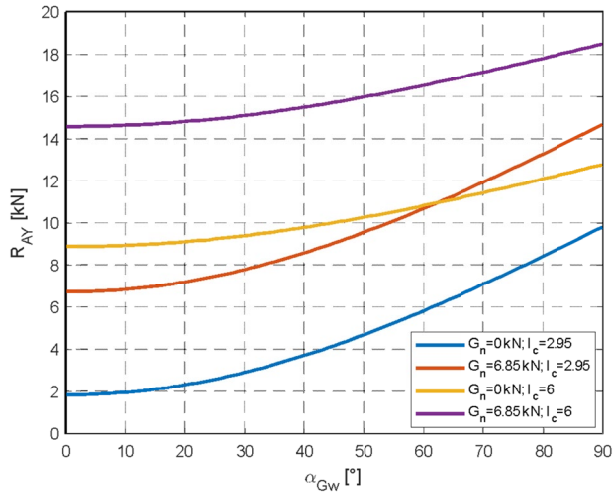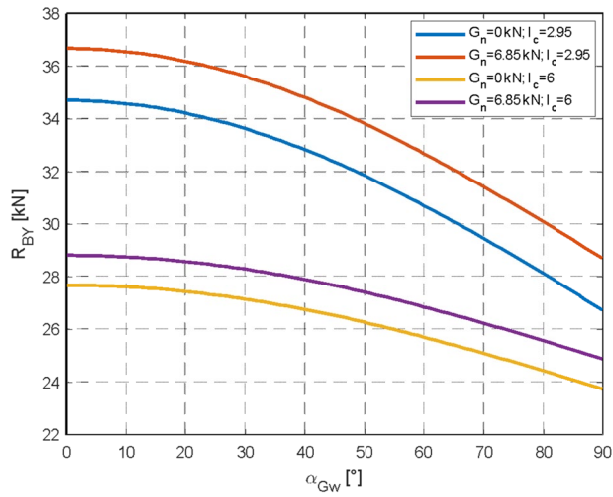
Fig. 17. Reaction value curve at points B as a function of the trajectory of the manipulator tip movement
in the vertical plane for the maximum manipulator's range $LZW_{z\max}$ and the arm tilt angle α_{GW},
where $G_n = 0$ and $G_n = 6.85$ kN ($l_c = l_1 + l_2 + l_3 = 2.95$ m and 6 m)

The final verification of the model and the calculations were carried out in a hard coal mine
excavation, where the manipulator's movement capabilities were tested (Fig. 18). This case was
considered in the support, stabilising foot (l_{GST}, α_{GST}) and boom system, with the possible tilt of
the boom reaching up to 90° and load up to 650 kg. As before, it was found that the stabilising
foot had no contact with the support when the arm tilt angle was not greater than 20° and the
counterweight reached 1500 kg.

Fig. 18. View of the MZT-M installed in an underground excavation

5. Conclusions

The aim of the developed manipulator model for supporting assembly works in underground excavations was to describe its essential functions (kinematics, stability) analytically, taking into account the counterweight mass. This model has been thoroughly described in previous publications [1,2]. A computer application was additionally written for this model, enabling the selection of parameters of the stabilising system of the manipulator. This article presents the computational capabilities of a computer program (application) and its use in practice.

Based on simulation and underground tests, it was found that the construction, design and working assumptions were fulfilled, which allows for recommendations of the manipulator for practical application in underground workings and the model and software – for design purposes.

References

[1] K. Krauze, R. Klempka, K. Mucha, T. Wydro, A. Kutnik, W. Hałas, P. Ruda, Determining the Stability of a Mobile Manipulator for the Transport and Assembly of Arches in the Yielding Arch Support. Energies **15**, 3170 (2022). DOI: https://doi.org/10.3390/en15093170

[2] K. Krauze, K. Mucha, T. Wydro, Wykorzystanie urządzeń mobilnych do montażu łuków obudowy chodnikowej. In: Mechanizacja, automatyzacja i robotyzacja w górnictwie 2021: monografia: praca zbiorowa / red. nauk. Krzysztof Krauze; Katedra Inżynierii Maszyn i Transportu. Wydział Inżynierii Mechanicznej i Robotyki. AGH Akademia Górniczo-Hutnicza. Wydawnictwa AGH, Kraków: 87-93 (2022).

[3] J. Korski, Temporary mechanized gate roof support in the YapiTec mine. IOP Conf. Ser.: Mater. Sci. Eng. 1134, 012002 (2021). DOI: https://doi.org/10.1088/1757-899X/1134/1/012002

[4] W. Zhang, G. Zhai, Z. Yue, T. Pan, R. Cheng, Research on Visual Positioning of a Roadheader and Construction of an Environment Map. Appl. Sci. **11** (11), 4968 (2021). DOI: https://doi.org/10.3390/app11114968

[5] Ch. Yan, W. Zhao, X. Lu, A Multi-Sensor Based Roadheader Positioning Model and Arbitrary Tunnel Cross Section Automatic Cutting. Sensors **19** (22), 4955 (2019). DOI: https://doi.org/10.3390/s19224955

[6] J. Janus, P. Ostrogórski, Underground Mine Tunnel Modelling Using Laser Scan Data in Relation to Manual Geometry Measurements. Energies **15** (7), 2537 (2022). DOI: https://doi.org/10.3390/en15072537

[7] M. Woszczyński, J. Rogala-Rojek, K. Stankiewicz, Advancement of the Monitoring System for Arch Support Geometry and Loads. Energies **15** (6), 2222 (2022). DOI: https://doi.org/10.3390/en15062222

[8] P. Cheluszka, Excavation of a layered rock mass with the use of transverse cutting heads of a roadheader in the light of computer studies. Archives of Mining Sciences **63**, 4, 871-890 (2018). DOI: https://doi.org/10.24425/ams.2018.124981

[9] P. Cheluszka, Optimization of the cutting process parameters to ensure high efficiency of drilling tunnels and use the technical potential of the boom-type roadheader. Energies **13** (24), 6597 (2020). DOI: https://doi.org/10.3390/en13246597

[10] A. Pytlik, Tests of steel arch and rock bolt support resistance to static and dynamic loading induced by suspended monorail transportation, Studia Geotechnica et Mechanica **41** (2), 81-92 (2019). DOI: https://doi.org/10.2478/sgem-2019-0009

[11] K. Krauze, Ł. Bołoz, K. Mucha, T. Wydro, The mechanized supporting system in tunnelling operations. Tunnelling and Underground Space Technology **113**, 103929 (2021). DOI: https://doi.org/10.1016/j.tust.2021.103929

[12] K. Krauze, K. Mucha, T. Wydro, A. Kutnik, W. Hałas, P. Ruda, D. Osowski, Operational Tests of a Modular Installation and Transport Assembly of Steel Arch Support in Underground Excavations. In: Multidisciplinary aspects of production engineering: monograph. Pt. 1, Engineering and technology / ed. Witold Biały. – Warszawa: Sciendo **4**, 1, 343-354 (2021). DOI: https://doi.org/10.2478/mape-2021-0031

[13] K. Drozd, A. Nieoczym, Dynamiczne obciążenie zawiesia generowane podczas jazdy z napędem własnym po trasie kolejki podwieszanej w wyrobisku (In Polish). Wydawnictwo Politechniki Lubelskiej, Lublin (2020).

[14] Ł. Bołoz, A. Kozłowski, Methodology for Assessing the Stability of Drilling Rigs Based on Analytical Tests. Energies 14, 8588 (2021). DOI: https://doi.org/10.3390/en14248588

[15] Ł. Bołoz, A. Kozłowski, W. Horak, Assessment of the Stability of Bev Lhd Loader. Management Systems in Production Engineering **30**, 4, 377-387 (2022). DOI: https://doi.org/10.2478/mspe-2022-0048

[16] P. Gospodarczyk, G. Stopka, P. Mendyka, Badania symulacyjne w projektowaniu innowacyjnego rozwiązania spągoładowarki (Simulation tests in designing an innovative solution of a dinting machine). Transport Przemysłowy i Maszyny Robocze: przenośniki, dźwignice, pojazdy, maszyny robocze, napędy i sterowanie, urządzenia pomocnicze **4**, 62-65 (2013),

[17] K. Kotwica, G. Stopka, P. Gospodarczyk, Simulation tests of new solution of the longwall shearer haulage system, IOP Conference Series: Materials Science and Engineering **679**, 012002, 1-8 (2019).
      DOI: https://doi.org/10.1088/1757-899X/679/1/012002